Published OnlineFirst November 7, 2014; DOI: 10.1158/1541-7786.MCR-14-0344-T

Oncogenes and Tumor Suppressors

Molecular Cancer Research

Survival Outcome and EMT Suppression Mediated by a Lectin Domain Interaction of Endo180 and CD147

Mercedes Rodriguez-Teja[1,2], Julian H. Gronau[1], Ai Minamidate[1], Steven Darby[3], Luke Gaughan[3], Craig Robson[3], Francesco Mauri[4], Jonathan Waxman[1], and Justin Sturge[1,5]

Abstract

Epithelial cell–cell contacts maintain normal glandular tissue homeostasis, and their breakage can trigger epithelial-to-mesenchymal transition (EMT), a fundamental step in the development of metastatic cancer. Despite the ability of C-type lectin domains (CTLD) to modulate cell–cell adhesion, it is not known if they modulate epithelial adhesion in EMT and tumor progression. Here, the multi-CTLD mannose receptor, Endo180 (MRC2/uPARAP), was shown using the Kaplan–Meier analysis to be predictive of survival outcome in men with early prostate cancer. A proteomic screen of novel interaction partners with the fourth CTLD (CTLD4) in Endo180 revealed that its complex with CD147 is indispensable for the stability of three-dimensional acini formed by nontransformed prostate epithelial cells (PEC). Mechanistic study using knockdown of Endo180 or CD147, and treatment with an Endo180 mAb targeting CTLD4 (clone 39.10), or a dominant-negative GST-CTLD4 chimeric protein, induced scattering of PECs associated with internalization of Endo180 into endosomes, loss of E-cadherin (CDH1/ECAD), and unzipping of cell–cell junctions. These findings are the first to demonstrate that a CTLD acts as a suppressor and regulatory switch for EMT; thus, positing that stabilization of Endo180–CD147 complex is a viable therapeutic strategy to improve rates of prostate cancer survival.

Implications: This study identifies the interaction between CTLD4 in Endo180 and CD147 as an EMT suppressor and indicates that stabilization of this molecular complex improves prostate cancer survival rates.

Visual Overview: http://mcr.aacrjournals.org/content/13/3/538/F1.large.jpg

Mol Cancer Res; 13(3); 538–47. ©2014 AACR.

Introduction

Epithelial-to-mesenchymal transition (EMT) is a reversible transdifferentiation program involving a switch from the apical-to-basal polarization of epithelial cells, which are adherent to each other and the basement membrane, to a detached mesenchymal-like phenotype that is highly motile and invasive (1). EMT is defined according to its different biologic contexts, including normal embryonic development (type I EMT), wound healing, tissue regeneration and organ fibrosis (type II EMT), or tumor progression (type III EMT; ref. 2). EMT has also been closely linked to the early stages of tumor development, following the finding that EMT-associated metastatic dissemination precedes detectable adenocarcinoma formation in glandular tissue (3). This strongly suggests that molecular triggers of EMT in normal epithelial layers should be prioritized as targets for the development of therapeutics that can prevent metastasis and improve cancer survival rates.

C-type lectin domains (CTLD) facilitate the Ca^{2+}-dependent interaction of cell surface receptors with carbohydrate moieties, playing critical roles in the innate immune response to pathogens, glycoprotein turnover, and modulation of cell–matrix and cell–cell interactions (4). In a biomarker study, we have previously revealed that the multi-CTLD receptor Endo180 (CD280, CLEC13E, KIAA0709, MRC2, TEM9, uPARAP) is highly expressed in cells with an EMT-like phenotype and correlated with Gleason score in prostate cancer (5). In the same study, Endo180 expression was observed in epithelial cells lining the ducts of glandular tissue affected by benign prostatic hyperplasia (BPH) or low-grade prostate cancer (5). Given that Endo180 expression and subcellular localization in constitutively recycling endosomes in mesenchymal-like tumor cells promote extracellular matrix (ECM) remodelling (6–10), disassembly of cell–cell and cell–matrix adhesions and cell motility (11, 12), and enhanced tumor growth (7), we hypothesized that these pro-EMT properties are negatively regulated in

[1]Department of Surgery and Cancer, Imperial College London, London, United Kingdom. [2]Departamento de Genética, Facultad de Medicina, Universidad de la República, Montevideo, Uruguay. [3]Northern Institute for Cancer Research, Newcastle University Medical School, Newcastle upon Tyne, United Kingdom. [4]Department of Medicine, Imperial College London, London, United Kingdom. [5]School of Biological, Biomedical and Environmental Sciences, University of Hull, Hull, United Kingdom.

Note: Supplementary data for this article are available at Molecular Cancer Research Online (http://mcr.aacrjournals.org/).

Corresponding Author: Justin Sturge, University of Hull, The Allam Building, Hull, HU6 7RX, UK. Phone: 44-0-1482-465316; Fax: 01482-465458; E-mail: j.sturge@hull.ac.uk

doi: 10.1158/1541-7786.MCR-14-0344-T

Published OnlineFirst November 7, 2014; DOI: 10.1158/1541-7786.MCR-14-0344-T

normal prostate epithelial cells (PEC). In accordance, this study has identified a novel EMT-suppressor complex between the fourth of eight CTLDs, CTLD4, in Endo180 and the cell adhesion modulator CD147 that is indispensible for PEC stability. We suggest that disruption of the suppressive Endo180–CD147 complex contributes to the marked decrease in survival attributed to Endo180 expression in low-to-intermediate grade (Gleason 5–7 score) prostate cancer. Hence, stabilization of the interaction between CTLD4 in Endo180 and CD147 is a promising therapeutic strategy that could suppress EMT and metastatic dissemination at the early stages of prostate adenocarcinoma formation.

Materials and Methods

Immunohistochemical analysis

The tissue biopsies on the NCLPC1 and NCLPC4 prostate cancer tissue microarrays (TMA) used in this study were obtained with consent and approved by the Research Ethics Committee of Newcastle University Medical School. Both TMAs were immunostained with the Endo180 mAb 39.10 (Supplementary Table S1; refs. 5, 7, 8) and a Histostain-Plus detection kit (Invitrogen). Images were collected using a Zeiss ChromaVision ACIS II automated slide scanner, an Olympus UPlanFLN 10X objective (N.A. = 0.30), and a Sony progressive CCD (charge-coupled device) color video camera. Immunohistochemical scores were calculated as percent positive cells (0 to 100) × staining intensity (0 to 3) with a cutoff score of 30 (range, 0–300) distinguishing positive from negative tumors. This immunohistochemical scoring system is in routine use in the Departments of Medicine and Surgery and Cancer at Imperial College London (13).

Cell culture, treatment, and morphologic analysis

RWPE-1, PC3, DU145, and B16-F10 were obtained from the American Type Culture Collection, where they were verified by short tandem repeat profiling and phenotypic analysis. BPH-1 cells were obtained from Dr. Simon Hayward (Vanderbilt University Medical Center) under a material transfer agreement and verified by phenotypic analysis. Cells were frozen in liquid nitrogen, and fresh aliquots were defrosted and tested for mycoplasma every three months (VenorGeM Mycoplasma Detection Kit) before their experimental use for up to ten passages. RWPE-1 cells were grown in complete keratinocyte serum-free media (Invitrogen). All other cells were grown in complete RPMI 1640 medium supplemented with 2 mmol/L L-glutamine, penicillin (50 U/mL) and streptomycin (50 μg/mL), and 10% v/v (PC3, DU145, and B16-F10) or 5% v/v (BPH-1) FCS. For three-dimensional (3D) acini (RWPE-1 or BPH-1) or 3D aggregate (DU145 or PC3) cultures, cells were seeded (5×10^3 per well) in 8-well chamber slides (Millipore Ltd.) precoated with Cultrex 3D Culture Matrix reduced growth factor reconstituted basement membrane (rBM) extract (#3445-005-01; Trevigen) and overlaid with growth medium + 2% v/v Cultrex rBM. Cells were transiently transfected with expression vectors or siRNA oligonucleotides (see Supplementary Methods; refs. 8, 11, 12). In brief, 24 hours after siRNAs transfection cells were transfected either with Endo180-Flag or Flag only, expression vectors were incubated overnight at 37°C with 5% v/v CO_2. Cells were seeded (5×10^3 per well) onto rBM, and remaining cells were lysed for assessment of knockdown efficiency using immunoblot analysis. Knockdown was sustained for the 4-day duration of the assay. Other treatments included addition of A5/158 or 39.10 mAbs, nonspecific negative control IgG (#ab37355; Abcam), GST, GST-CTLD2, or GST-CTLD4 (see Supplementary Methods) to the culture medium with daily replacement. A blinded manual scoring approach (two independent scorers) was used to calculate the percentage of acini containing ≥4 cells for each condition relative to the control (set at 100%).

Immunoblotting and immunofluorescent staining

Immunoblotting and immunofluorescent staining of monolayers and 3D cultures were carried out with primary antibodies (Supplementary Table S1) and appropriate horseradish peroxidase–conjugated or AlexaFluor-conjugated secondary antibodies (8, 11, 12, 14). For immunoblots, relative signal intensities for each band were quantified using Image J (Version 1.42q), adjusted for loading (GAPDH or ERK-2), and normalized against untreated samples (relative levels, 1). For immunofluorescent staining, phalloidin-AlexaFluor-488 was added to the secondary antibody dilution to visualize F-actin fibers. TO-PRO-3 iodide or 4′,6-diamidino-2-phenylindole (DAPI) were used as nuclear counterstains. Images were acquired using an Axiovert S100 epifluorescent/brightfield microscope with a Zeiss N-Achroplan 20× objective (N.A. = 0.45), a Hamamatsu Orca AG high-end cooled CCD imaging camera, and Metamorph software operating system (Molecular Devices); or a Zeiss LSM 510 laser scanning confocal microscope with Zeiss Plan-Apochromat 63× and 40× oil immersion DIC objectives (N.A. = 1.4), a Hamamatsu CCD imaging camera for widefield imaging on an Axioplan 2 mounting, and Zeiss LSM 510 Meta operating system. Images were equally adjusted for brightness and contrast using Adobe Photoshop CS4 (Version 11.0.2) or Zeiss LSM Image Browser (Version 4.2.0.121).

Antibody array, pull-down assays, and immunoprecipitation

ARY012 antibody arrays (R&D Systems) were incubated with GST or GST-CTLD4 elutes following the manufacturer's protocol. Relative signal intensities of duplicate spots (mean ± SD) were quantified (Image J version 1.42q) and normalized against the internal positive control. For pull-down assays, GST and GST-fusion proteins conjugated to glutathione-sepharose beads were incubated with cell lysates (4°C, 12 hours), washed in GST-lysis buffer and centrifuged at 14,000 rpm (4°C, 2 minutes; 5×), and denatured (95°C, 5 minutes). Ectopically expressed Endo-Flag chimeric protein (Supplementary Methods) was immunoprecipitated from whole cell lysates using a FLAG-tagged protein immunoprecipitation kit (#FLAGIPT1; Sigma-Aldrich). Pulled down and immunoprecipitated proteins were resolved using SDS-PAGE and immunoblotted (see above).

Statistical analysis

SPSS (Version 19) was used to create Kaplan–Meier plots (censored to account for any patient withdrawals before the final outcome is observed) and to perform log-rank, Breslow, and Tarone–Ware analyses and Student *t* tests (two-tailed, $\alpha = 0.05$).

Results

Endo180 expression in early prostate neoplasms decreases survival

Endo180 was analyzed for its contribution to clinical outcome using prostate cancer TMAs that were established at the University

Published OnlineFirst November 7, 2014; DOI: 10.1158/1541-7786.MCR-14-0344-T

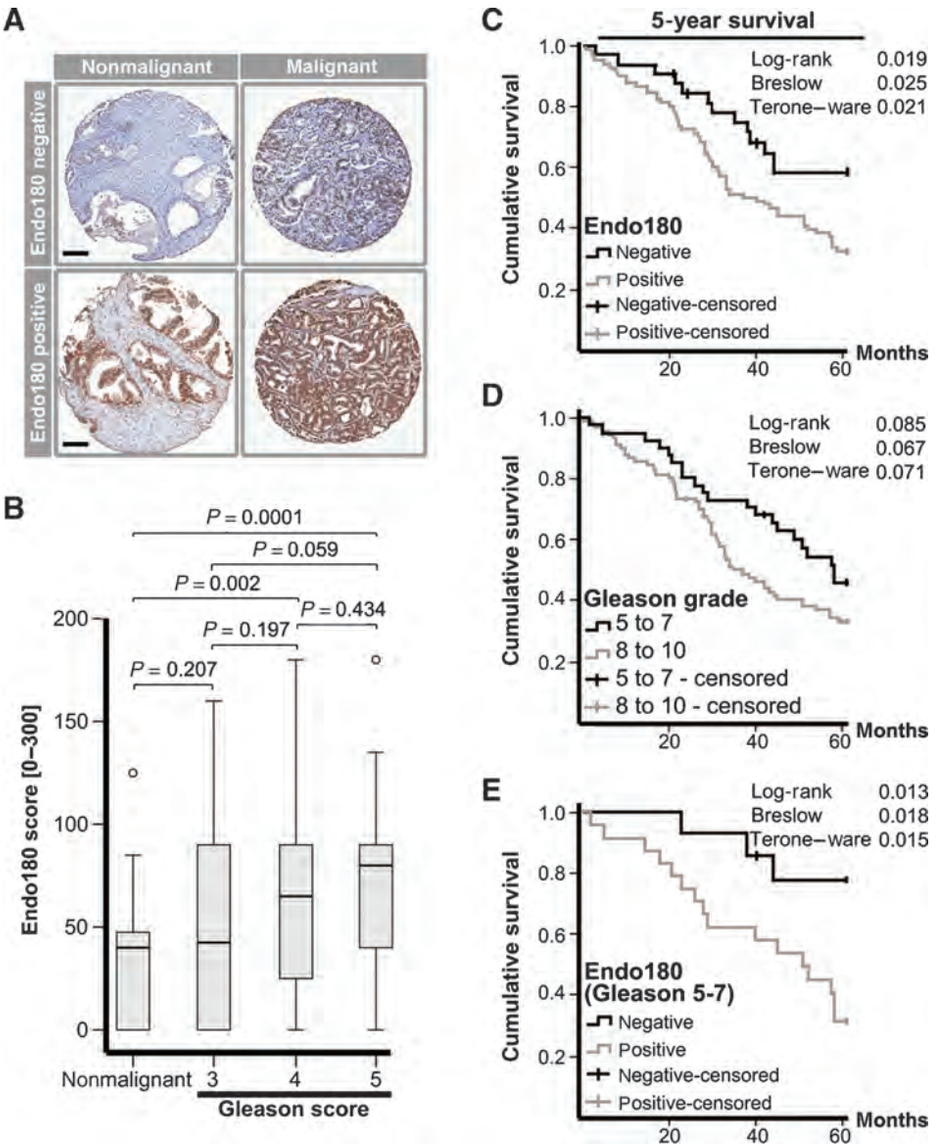

Figure 1.
Endo180 predicts overall survival. A, Endo180 immunostaining in nonmalignant and malignant prostate tissue; magnification, ×10; scale bar, 200 μm. B, box and whiskers plot show Endo180 correlation with Gleason score; total range, interquartile distribution, outliers (open circles), and median value (horizontal line) of Endo180 scores for NCLPC4 TMA: nonmalignant tumor-adjacent tissue ($n = 35$); Gleason score 3 ($n = 36$), 4 ($n = 58$), and 5 ($n = 48$). The Kaplan–Meier five-year survival analysis of NCLPC1/4 TMAs ($n = 157$) for (C) Endo180-negative (black line) and -positive (gray line) tumors; (D) Gleason score 5–7 (black line) and 8–10 (gray line) tumors; and (E) Endo180-negative (black line) and -positive (gray line) tumors in the Gleason 5–7 subset; *P* values shown for log-rank, Breslow, and Tarone–Ware tests.

of Newcastle. In accordance with our earlier findings using a commercial TMA (5), high Endo180 expression was observed in the epithelium, with lesser staining in the stroma, of nonmalignant tumor-adjacent BPH tissue cores (Fig. 1A and Supplementary Table S2); and significant increases in Endo180 expression in PECs in Gleason score 4 and 5 tumor tissue cores compared with nonmalignant tumor-adjacent BPH (Fig. 1B).

The Kaplan–Meier analysis identified Endo180 as an independent predictor of poor prognosis, with only 39% (13/33) deaths recorded after five years for Endo180-negative tumors compared with 65% (60/93) for Endo180-positive tumors [Fig. 1C; Supplementary Table S3 shows deaths (censored) after three, five, seven, and ten years, $P < 0.03$]. There was a marginal difference in the five-year overall survival rate of men with low-to-intermediate grade (Gleason sum score 5–7) versus high-grade (Gleason sum score 8–10) prostate cancer (Fig. 1D and Supplementary Table S3, $P > 0.07$). For low-to-intermediate grade tumors, there were 21% (3/14) and 67% (16/24) respective deaths recorded in Endo180-negative and -positive cases (Fig. 1E and Supplementary Table S3, $P < 0.02$), which despite the relatively low number of patient numbers in this subset indicates that Endo180 expression in these earlier stage neoplasms has a major impact on clinical outcome.

Endo180 is necessary for prostate gland acinar stability

We hypothesized that the significant clinical impact of Endo180 expression at the early stages of prostate cancer results from the negative regulation of its proinvasive function being lost. To determine if Endo180 contributes to epithelial stability, we genetically silenced the receptor during 3D PEC acinar morphogenesis. In accordance, the loss of Endo180 induced scattering of RWPE-1 and BPH-1 cells into the surrounding rBM (Supplementary Fig. S1A and S1B), without affecting their cell cycle or viability (Supplementary Fig. S2A–S2C), revealing that a critical biologic

Published OnlineFirst November 7, 2014; DOI: 10.1158/1541-7786.MCR-14-0344-T

function of the receptor in normal glandular PECs is to stabilize their adherence to each other and the basement membrane to help maintain their apical-to-basal polarity.

Endo180 is an uptake receptor for collagen cleavage products generated by the proteolytic activity of membrane type-1 metalloproteinase (MT1-MMP; ref. 15). To test whether silencing of MT1-MMP has a similar effect on acinar architecture to Endo180 knockdown, we depleted MT1-MMP from 3D cultures of RWPE-1 and BPH-1 cells (Supplementary Fig. S1A and S1B). The results confirmed that, unlike Endo180, MT1-MMP is not required for the maintenance of PEC acinar homeostasis. In addition, silencing of Endo180 in 3D aggregates formed by metastatic prostate tumor cells (PTC; PC3 and DU145) did not induce scattering into the surrounding rBM (Supplementary Fig. S1A and S1C), which suggests that Endo180-dependent stabilization of cell–cell adhesions is a molecular mechanism that is exclusive to nontransformed prostatic epithelia.

Endo180 siRNA oligonucleotides #1 and #2 respectively bind to the 3′ untranslated region noncoding and mRNA coding regions of the gene (Fig. 2A); therefore, oligonucleotide #1 is not able to silence ectopically expressed Endo180-Flag (Fig. 2B). We used this distinguishing feature of these two oligonucleotides to determine if ectopic expression of Endo180 during endogenous receptor silencing can reverse this dramatic change in acinar architecture. Indeed, ectopic Endo180-Flag expression in PECs rescued the effect of Endo180 siRNA oligonucleotide #1, but not #2, on acinar cell–cell stability (untreated control = 100% fully formed acini; control siRNA = 88.0% ± 18.7%; oligonucleotide #1 = 88.7% ± 24.9%; oligonucleotide #2 = 29.6% ± 5.5%; Fig. 2C and D). As expected, ectopic expression of Flag alone did not rescue the inhibitory effect of either Endo180 siRNA oligonucleotide (untreated control = 100%; control siRNA = 97.7% ± 25.8%; oligonucleotide #1 = 24.1% ± 1.3%; oligonucleotide #2 = 23.2% ± 6.2%; Fig. 2C and D). Acinar morphogenesis by RWPE-1-Flag and RWPE-1-Endo180-Flag cells treated with Endo180 siRNA oligonucleotide #1 was significantly different (Student test: $P = 0.01$, two-tailed; Fig. 2D). Moreover, Endo180-Flag was clearly localized to the basolateral membrane of PECs treated with Endo180 siRNA oligonucleotide #1 (Fig. 2C). These data establish that loss of Endo180 from the plasma membrane

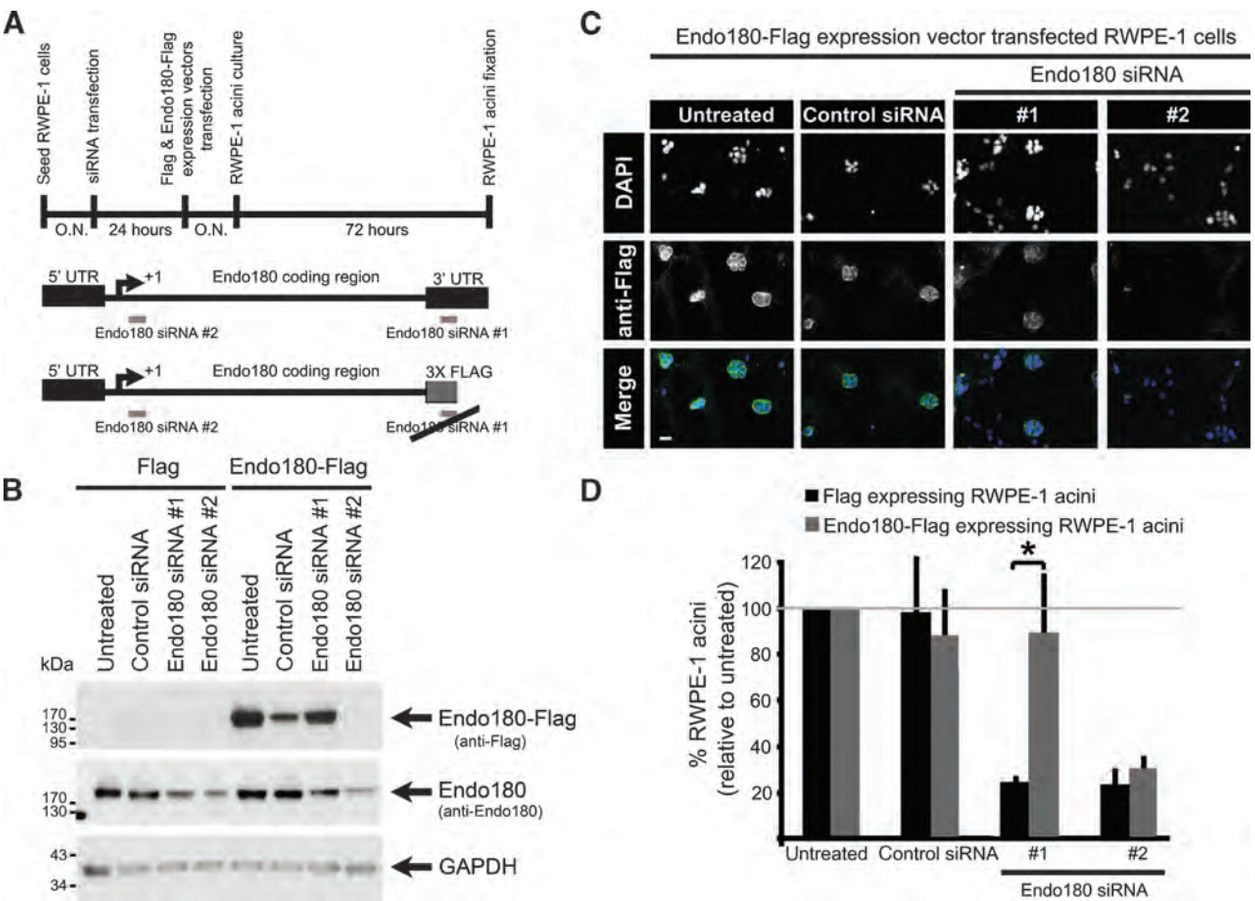

Figure 2.
Membrane-localized Endo180 is indispensable for cell–cell adhesion. A, schematic of experimental timeline and annealing sites for Endo180 siRNA oligonucleotides #1 and #2. B, immunoblots show Endo180-Flag, endogenous Endo180, and GAPDH levels in RWPE-1 cells expressing Flag or Endo180-Flag that had been untreated or treated with control siRNA or Endo180 siRNA oligonucleotides #1 and #2; MW markers, kDa. C, RWPE-1 cells cultured for three days in rBM stained with DAPI (blue) and anti-Flag to detect Endo180-Flag (green); magnification, ×20; scale bar, 20 μm. D, average ± SD percentage of fully formed acini by cells expressing Endo180-Flag (gray bars) or empty vector (black bars); untreated cells = 100%; *, significant difference, $P = 0.01$.

Published OnlineFirst November 7, 2014; DOI: 10.1158/1541-7786.MCR-14-0344-T

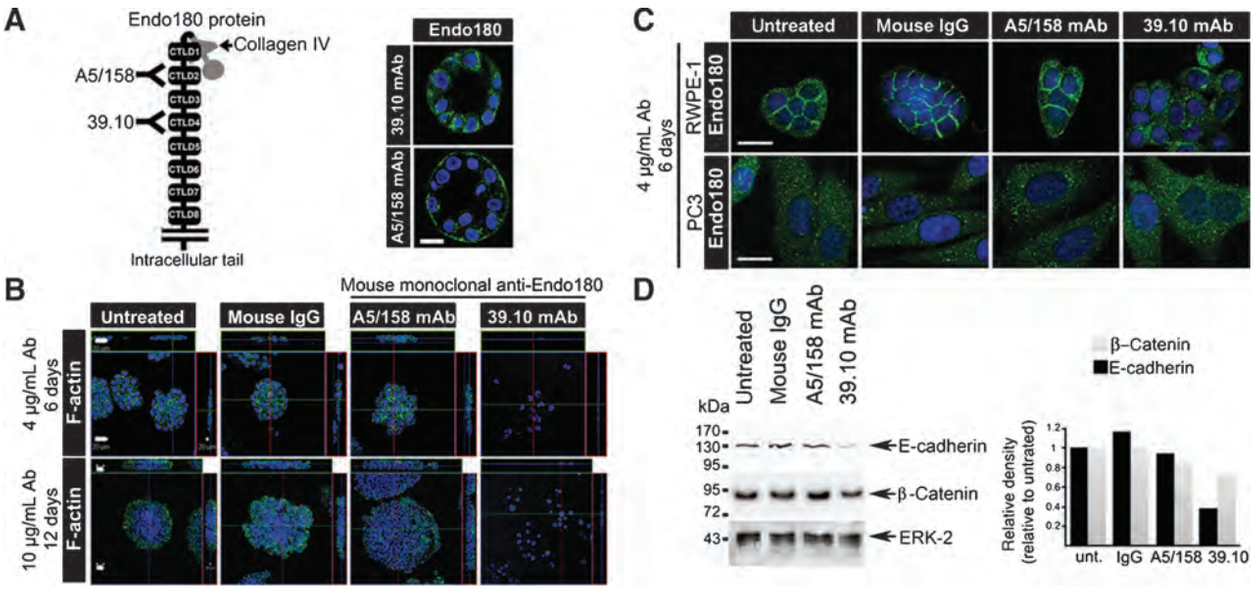

Figure 3.

CTLD4 in Endo180 is required for cell–cell adhesion. A, epitopes in human Endo180 ectodomain recognized by A5/158 and 39.10 mAbs and corresponding immunostaining in RWPE-1 acini (inset); magnification ×63; scale bar, 10 µm. B, RWPE-1 cells cultured in rBM without (untreated) or with mouse IgG, A5/158, and 39.10 for six or 12 days stained with phalloidin (green) and TO-PRO-3 (blue); magnification, ×40; scale bar, 20 µm. C, RWPE-1 and PC3 cell monolayers cultured without (untreated) or with mouse IgG, A5/158, or 39.10 for six days stained with A5/158 (green) and DAPI (blue); magnification, ×63; scale bar, 20 µm. D, immunoblots show E-cadherin, β-catenin, and ERK2 levels in RWPE-1 cells untreated or treated with IgG control or A5/158 and 39.10; MW markers, kDa. Graph shows relative levels of E-cadherin (black bars) and β-catenin (gray bars) adjusted against ERK2 levels and normalized against untreated cells (relative levels = 1).

in epithelial cell monolayers may be a driving force behind the switch to an EMT-like phenotype and the dissemination of cells into the surrounding matrix.

CTLD4 in Endo180 receptor modulates glandular epithelial cell–cell adhesion

Differential staining patterns for Endo180 with different mAbs indicated that two subcellular pools of the receptor are present in PEC acini. The first subcellular pool of Endo180 is localized at the basolateral membrane and recognized by A5/158 mAb, whereas the second is localized in endosomes and recognized by 39.10 mAb (Fig. 3A). Treatment with the two antibodies revealed that incubation with 39.10 mAb, but not A5/158, resulted in the same effect as Endo180 silencing by scattering PECs into the surrounding rBM (Fig. 3B). Epitope mapping has confirmed that A5/158 mAb binds to CTLD2 in Endo180 (11). Using a similar epitope mapping approach that involved immunoblot analysis of truncated forms of Endo180 with successive deletions in each of its domains down to CTLD5, it was confirmed that 39.10 mAb binds to CTLD4 (Supplementary Fig. S3A and S3B). This indicates that CTLD4, but not CTLD2, is required for PEC adhesion. The inability of 39.10 mAb to promote cell scattering from 3D aggregates formed by metastatic PTCs (Supplementary Fig. S4) is likely to be the result of constitutive recycling of the receptor from the plasma membrane and its localization to endosomes in transformed mesenchymal-like cells (Fig. 3C; refs. 11, 12).

The strong localization of Endo180 observed at the basolateral membrane of untreated or mouse IgG–treated PEC monolayers was lost following treatment with 39.10 mAb, but not A5/158 mAb, resulting in most of the receptor being localized to endosomes (Fig. 3C). In line with the induction of programmed EMT, the treatment of PECs with 39.10 mAb resulted in a decrease in total cellular levels of E-cadherin (0.3-fold) and β-catenin (0.7-fold; Fig. 3D). In contrast, levels of these core cell–cell adhesion components were unaffected by treatment with A5/158 mAb (E-cadherin: 0.9-fold; β-catenin: 0.9-fold) or IgG control (E-cadherin: 0.8-fold; β-catenin: 1.0-fold; Fig. 3D). Again the disseminated PECs retained their ability to survive, as confirmed by the lack of effect of 39.10 mAb on their cell cycle and viability (Supplementary Fig. S2D–S2G).

We next considered the hypothesis that the inability of 39.10 mAb to recognize Endo180 localized at the plasma membrane is due to CTLD4 epitope being masked by unknown interaction partner(s). We also predicted that treatment with soluble GST-CTLD4 would disrupt epithelial cell–cell contacts by imposing a dominant-negative effect on the unknown interaction partner(s) (Fig. 4A). To test this hypothesis, we generated GST-CTLD2 and GST-CTLD4 chimeric proteins (Fig. 4B) and used them as competing agents for CTLD2 and CTLD4 ligands during PEC acinar morphogenesis. In agreement with antibody-blocking experiments, GST-CTLD4, but not GST-CTLD2, induced scattering of RWPE-1 and BPH-1 cells into the surrounding rBM (Fig. 4C) without affecting cell viability (Supplementary Fig. S2H).

CTLD4 in Endo180 receptor interacts with highly glycosylated CD147

Proteomic analysis of interaction partners eluted from GST-CTLD4–conjugated sepharose beads that had been incubated with PEC whole cell lysates revealed that Endo180 forms a molecular complex with CD147 and CD36 (Fig. 4D and E). Given that CD147 is associated with prostate cancer progression (16), we decided to explore its cooperative role with Endo180.

Published OnlineFirst November 7, 2014; DOI: 10.1158/1541-7786.MCR-14-0344-T

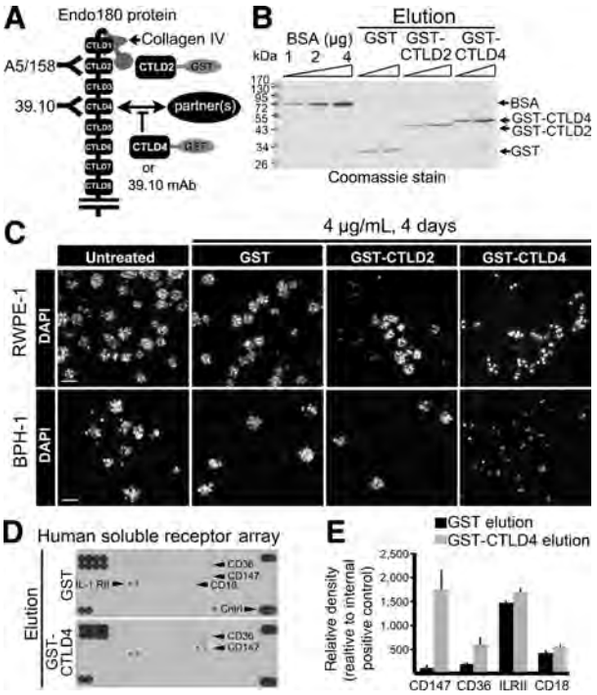

Figure 4.
CTLD4-dependent cell–cell adhesion is associated with its novel interaction partner CD147. A, epitopes in human Endo180 ectodomain recognized by A5/158 and 39.10 mAbs and corresponding GST-CTLD2 and GST-CTLD4 chimeric proteins generated. B, coomassie stain of elutes containing purified GST, GST-CTLD2, GST-CTLD4, and BSA; MW markers, kDa. C, RWPE-1 and BPH-1 cells cultured in rBM without (untreated) or with purified GST, GST-CTLD2, or GST-CTLD4 (4 μg/mL a day for four days) stained with DAPI; magnification, ×20; scale bar, 50 μm. D, GST-CTLD4 and GST whole cell lysate pull-down assays analyzed using an array containing 57 antibodies printed in duplicate. Proteins of interest eluted (black arrows) include CD36/SR-B3 (Entrez gene #948), CD18/integrin β_2 (Entrez gene #3689), IL1RII (Entrez gene #7850), and CD147/EMMPRIN (Entrez gene #682). E, average relative density ± SD (pixels/unit area) of duplicate spots (GST, black bars; GST-CTLD4, gray bars) normalized against internal positive control (+Cntrl, panel D).

Endo180-CTLD4 and CD147 complex formation was further demonstrated by the ability of GST-CTLD4, but not GST-CTLD2 or GST alone, to bind to the highly glycosylated and active form of CD147 (Supplementary Fig. S5A). Anti-Flag immunoprecipitation of highly glycosylated CD147 from PECs transfected with Endo180-Flag also consolidated its interaction with Endo180 (Supplementary Fig. S5B). Conversely, E-cadherin, β-catenin, and ZO-1 were not detected in Endo180-Flag immunoprecipitates (Supplementary Fig. S5C), suggesting that Endo180 is not incorporated into adherens and tight junction protein complexes. This is not surprising given that Endo180 is weakly localized in lateral cell–cell junctions and strongly localized at the basal plasma membrane of PEC acini (Fig. 3A). In agreement, E-cadherin and β-catenin were not identified as Endo180 interaction partners (Supplementary Fig. S5C).

Endo180–CD147 complex disassembly promotes EMT

Glycosylation of CD147, following its disassociation from caveolin-1, promotes its self-aggregation, stabilization at the plasma membrane and enhanced cell adhesion (17). Based on the ability of highly glycosylated CD147 localized at the plasma membrane to promote cell adhesion, we determined whether its interaction with CTLD4 in Endo180 was responsible for cell–cell adhesion stability in PEC acini. Incubation of PECs with increasing concentrations of the dominant-negative GST-CTLD4 construct decreased the ratio of high/low glycosylated CD147 present in whole cell lysates (2 μg/mL: ratio = 0.71; 4 μg/mL: ratio = 0.25) compared with untreated cells (ratio = 1.0) or cells treated with GST alone (ratio = 1.16) as determined by semiquantitative immunoblot analysis (Fig. 5A). The same treatment did not induce any change in the glycosylation status of CD147 in PTC's (Fig. 5A). Similar to treatment with GST-CTLD4, treatment with 39.10 mAb also decreased the ratio of high/low glycosylated CD147 in PECs (control IgG treatment: ratio = 1.85; 39.10 mAb treatment: ratio = 0.16) but not PTCs (Fig. 5B). The shift in the glycosylation status of CD147—from high to low—induced by GST-CTLD4 in PECs correlated CD147 internalization (Fig. 5C, arrowheads) and unzipping of adherens junctions (Fig. 5C, arrows). These results

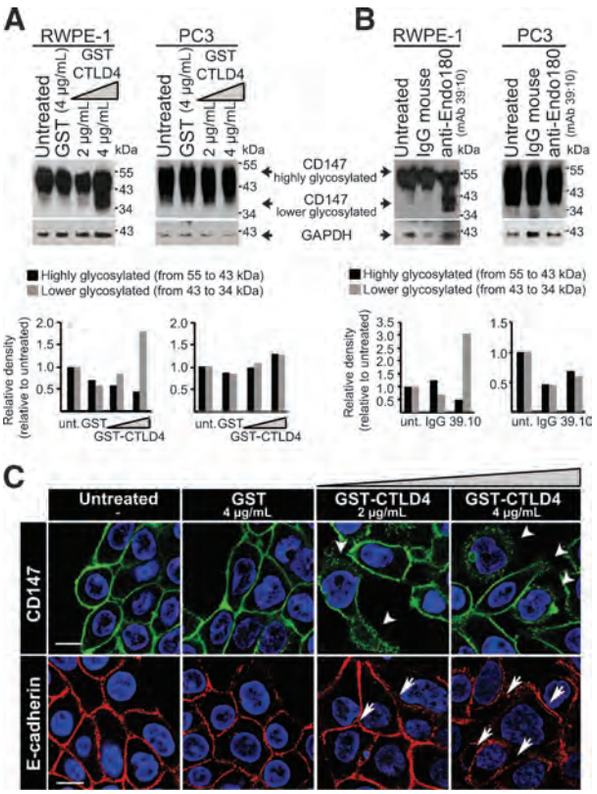

Figure 5.
Endo180–CD147 complex disruption decreases glycosylation and promotes internalization of CD147 with unzipping of cell–cell junctions. Immunoblots of CD147 (high/low glycosylated forms indicated) and GAPDH levels in RWPE-1 and PC3 whole cell lysates following treatment with GST or GST-CTLD4 (A) and mouse IgG or 39.10 mAb (B); MW markers, kDa. Graph shows relative amount of CD147 with high (above 43 kDa, black bars) and low (below 43 kDa, gray bars) glycosylation compared with untreated cells adjusted against GAPDH. C, immunostaining of CD147 (green), E-cadherin (red), and TO-PRO-3 (blue) in RWPE-1 monolayers; arrowheads, cells with internalized CD147; arrows, unzipped cell–cell junctions; magnification, ×63; scale bar, 10 μm.

Published OnlineFirst November 7, 2014; DOI: 10.1158/1541-7786.MCR-14-0344-T

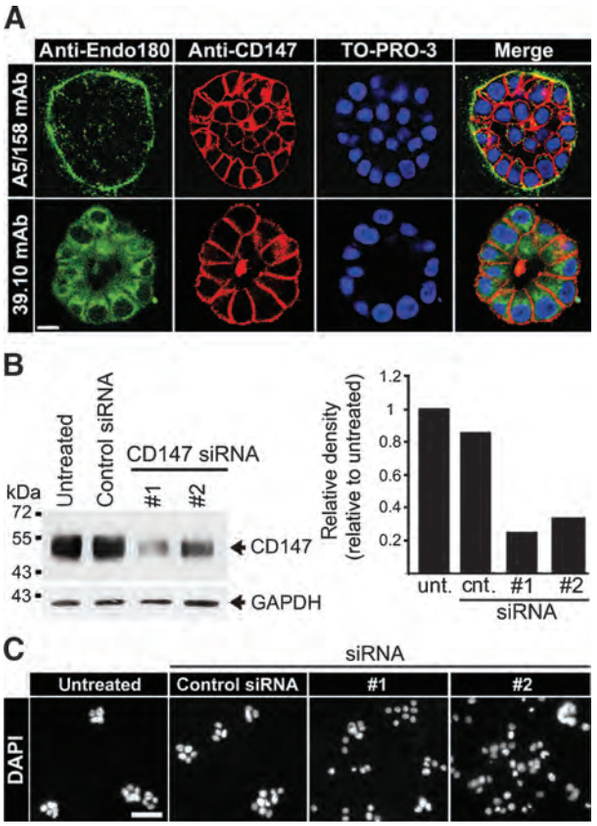

Figure 6.
CD147 colocalizes with Endo180 at the basolateral membrane and is required for cell–cell adhesion. A, Endo180 [green, A5/158 mAb (IgG_1) and 39.10 mAb (IgG_1)], CD147 [red, anti-human CD147 mAb (IgG_{2ak})], and TO-PRO-3 (blue) immunostaining of RWPE-1 cells cultured for six days in rBM; magnification, ×63; scale bar, 10 μm. B, immunoblots show endogenous CD147 and GAPDH levels in RWPE-1 cells treated with control or CD147 (#1 and #2) siRNA oligonucleotides; MW markers, kDa. Graph shows CD147 levels adjusted against GAPDH and normalized against untreated control (relative levels = 1). C, cells seeded on rBM for three days stained with DAPI; magnification, ×20; scale bar, 50 μm.

consolidate the link between Endo180–CD147 complex disruption and the initiation of EMT in prostate epithelial monolayers.

To shed more light on our newly established model of Endo180–CD147-dependent cell–cell adhesion and EMT suppression, we costained PEC acini with anti-CD147 and A5/158 or 39.10 mAbs. The findings revealed that CD147 localizes with Endo180 at the basal plasma membrane but not in endosomes (Fig. 6A). Finally, we demonstrated that CD147 silencing (Fig. 6B) also scattered PECs into their surrounding rBM (Fig. 6C), which is in agreement with the pro-EMT effect observed following their treatment with Endo180 siRNA oligonucleotides (Supplementary Fig. S1B) 39.10 mAb (Fig. 3B) and GST-CTLD4 (Fig. 4C).

Discussion

The revelation that Endo180 interacts with, and stabilizes, highly glycosylated CD147 at the plasma membrane of normal PECs, and that destabilization of the complex leads to type III EMT, establishes a new type of molecular trigger for the development of invasive prostate cancer. The findings of this study also confirm that, similar to the upregulation of CD147 (5, 16), the increased expression of Endo180 is correlated with increasing Gleason score (Fig. 1B) and has prognostic value as an independent predictor of overall survival (Fig. 1C). Surprisingly, the Kaplan–Meier analysis revealed that Endo180 is a stronger predictor of survival than Gleason score. However, the cutoff between Gleason 5–7 and Gleason 8–10 used may have skewed the latter outcome given that ≤Gleason 7 (3+4) and ≥Gleason 7 (4+3) scores confer differences in overall survival (18). Future studies using larger patient cohorts are needed to determine if Endo180 expression can differentially affect the survival of men with low (≤Gleason 6) and intermediate [Gleason 7 (3+4)] risk tumors.

Although previous work has suggested that there is a close association between Endo180 expression and an EMT-like phenotype in transformed cells derived from breast (7), pancreatic (10), and prostate (5) cancer, the divergent mechanistic roles of Endo180 in this fundamental process had not been appreciated. Endo180 and CD147 have both been correlated with low levels of E-cadherin in tumor tissue, and both are under the transcriptional regulation of the core EMT trigger TGFβ (7, 8, 19, 20). In an aligned study, we have demonstrated that the stiff microenvironment associated with advanced glycation endproduct accumulation and collagen crosslinking of the basement membrane in the prostate gland is sufficient to activate an EMT-like phenotype in PEC acini by forcing the relocalization of Endo180 into endosomes and initiating an Endo180-dependent contractile signaling cascade that promotes cell invasion (21). Indeed, ECM stiffness has been identified as a regulator that can release matricellular TGFβ in a number of pathologies (22). Considering the findings reported here, we believe that the TGFβ–Endo180 axis is a central regulatory pathway that controls the induction of EMT in human glandular tissue. It is possible that the EMT suppressor function of membrane-bound Endo180 in nononcogenic epithelia, and the prometastatic function of Endo180 in endosomes in newly established tumors, underpins the paradoxical roles of TGFβ as a suppressor and promoter of cancer progression (23). Our future investigations will be focused on unraveling the complex environmental factors and mechanisms—including tissue hypoxia, age-dependent ECM stiffness, and obesity-associated inflammation—that lie upstream of Endo180–CD147 complex disruption and can drive the progression of indolent lesions to aggressive neoplasms in prostate and other glandular epithelia. It will also be important to establish which other specific EMT-associated events, in addition to the downregulation of E-cadherin, are triggered by Endo180–CD147 complex disruption. This analysis could include evaluation of master regulators of EMT, including Snail, Slug, Twist, Zeb, and microRNAs (24).

The characterization of Endo180 for its carbohydrate-binding capacity has so far only included an *in vitro* analysis that identified CTLD2 as the sole CTLD possessing lectin activity (25). The finding here that CTLD4 in Endo180 binds to highly glycosylated CD147 in 3D acini culture suggests that it also behaves as an active lectin in an *in vivo* context. Interestingly, *in vitro* analysis and *in vivo* evidence have confirmed that lectin activity also resides in the fourth CTLD of the related mannose receptor (26), which points toward an evolutionary basis for the position of this domain in multi-CTLD receptors.

Published OnlineFirst November 7, 2014; DOI: 10.1158/1541-7786.MCR-14-0344-T

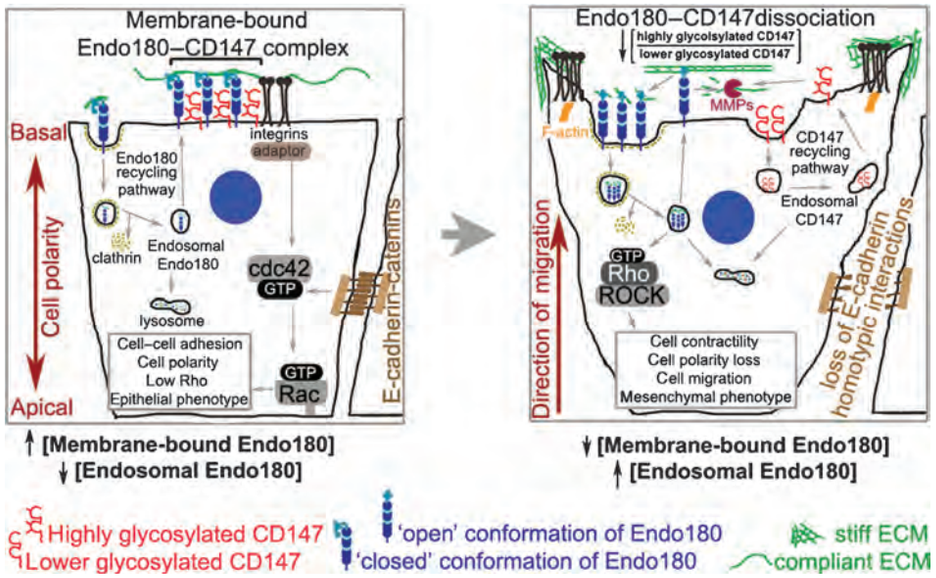

Figure 7.
Schematic showing how Endo180–CTLD4 and CD147 complex stabilizes normal epithelial apical-to-basal cell polarity. Endo180–CTLD4 and CD147 complex disruption results in Endo180 internalization via clathrin-dependent endocytosis and CD147 internalization via a clathrin-independent mechanism (35). Endo180-containing endosomes generate spatiotemporal contractile signals that destabilize cell–cell adhesions, increase cell–matrix adhesion turnover, and endow disseminated cells with promigratory and chemotactic properties (12). CD147 and Endo180 remodel the ECM via respective activation of MMPs (36) and participation in collagen remodeling (7, 8, 14, 32, 34) via their distinct cellular pathways.

Interestingly, two other cell surface receptors that each have a single CTLD and confined to the tumor vasculature are being considered as molecular targets of antiangiogenics for indirect treatment of solid tumors. The first, CLEC14A (EGFR-5), is exclusively expressed by vascular endothelial cells and promotes cell–cell adhesion and neo-angiogenesis via its single CTLD (27–29). The second, endosialin (CD248, TEM-1), is expressed by stromal fibroblasts and pericytes and can promote tumor angiogenesis and growth (30, 31). Our study now opens the way for CTLD4 in Endo180 to be characterized for its cooperative role with CD36 (Fig. 4D) and other glycosylated ligands and *bona fide* lectin activity in addition to its exploitation as a therapeutic target in metastatic cancer.

The importance of CTLD4 for the formation of the suppressive Endo180–CD147 complex in PECs was not uncovered in Endo180$^{\Delta Ex2\text{-}6/\Delta Ex2\text{-}6}$ mice that express a truncated form of the Endo180 receptor, including an intact CTLD4, and reach adulthood (32, 33). Nevertheless, our analysis of prostate tissue from adult Endo180$^{\Delta Ex2\text{-}6/\Delta Ex2\text{-}6}$ mice has revealed that a significant architectural change occurs that closely recapitulates prostatic intraepithelial neoplasia, a common precursor for invasive prostate cancer (M. Rodriguez-Teja and colleagues; unpublished data). This finding can be explained by experimental evidence that suggests constitutively exposed CTLD2 in Endo180$^{\Delta Ex2\text{-}6/\Delta Ex2\text{-}6}$ mice binds to glycated collagen (34) to promote mechanotransduction and cell invasion (M. Rodriguez-Teja and colleagues; unpublished data). Given that only 3.5% of CD147$^{-/-}$ mice reach adulthood due to failed blastocyst implantation (35), it will be of considerable interest to determine if targeted deletion of CTLD4 or full genetic ablation of Endo180 results in a developmental defect. The impact of Endo180 silencing and Endo180–CD147 complex disruption in different glandular epithelia also needs exploration using appropriate *in vivo* models.

Together with previous findings, this study establishes a new mechanism for the early stages of tumor formation that involves (a) Endo180–CTLD4 and CD147 complex disruption; (b) Endo180 internalization into the cytoplasm via clathrin-dependent endocytosis; (c) CD147 internalization into the cytoplasm via a clathrin-independent mechanism (36); and (d) generation of spatiotemporal contractile signals (RhoA-ROCK-MLC2) from Endo180-containing endosomes that destabilize cell–cell adhesions, increase the turnover of cell–matrix adhesions, and endow disseminated cells with the capacity to migrate via ligand-specific chemotactic mechanisms toward distant sites (refs. 11, 12; Fig. 7). It is also plausible that CD147 and endosomal Endo180 help to coordinate ECM turnover via their respective activation of MMPs (37) and participation in collagen remodeling (7, 8, 14, 34). In addition to inducing Endo180 internalization, Endo180–CTLD4 and CD147 complex disruption deglycosylates and internalizes CD147. Hence, it is possible that Endo180 stabilizes CD147 at the plasma membrane by competing with its negative regulator caveolin-1 (17).

Progression toward metastatic castrate-resistant prostate cancer and the contribution of aberrant androgen signaling to this process remain a major therapeutic challenge (38). Negative androgen receptor (AR) status is correlated with the expression of Endo180 in breast cancer (7). This suggests that dysregulation of the androgen axis and AR signaling may act as a trigger for Endo180 expression and enhanced metastatic potential. A putative role for Endo180 in androgen-independent prostate cancer is further consolidated by its absence from the androgen-dependent and noninvasive LNCaP prostate cancer cell line (8). Together, these observations set a precedent for investigating the interaction between AR signaling and the Endo180 axis.

In combination with the continued validation of soluble Endo180 in serum as a highly sensitive and specific biomarker for metastatic disease (39), the findings of this study suggest that strategies for antimetastatic therapy should (a) promote stabilization of the suppressive complex between CTLD4 in Endo180 and CD147 at the plasma membrane, in the case of indolent diseases like BPH, and (b) exclusively target endosomal Endo180, in the case of aggressive tumors. We predict that the aligned introduction of Endo180 as a prognostic marker and therapeutic target will have a significant impact on the prognosis

and prevention of metastasis in prostate cancer and could also be of benefit in the management of other types of carcinoma.

Disclosure of Potential Conflicts of Interest

No potential conflicts of interest were disclosed.

Authors' Contributions

Conception and design: M. Rodriguez-Teja, J. Waxman, J. Sturge
Development of methodology: M. Rodriguez-Teja, J. Sturge
Acquisition of data (provided animals, acquired and managed patients, provided facilities, etc.): M. Rodriguez-Teja, J.H. Gronau, S. Darby, L. Gaughan, J. Sturge
Analysis and interpretation of data (e.g., statistical analysis, biostatistics, computational analysis): M. Rodriguez-Teja, J.H. Gronau, S. Darby, F. Mauri, J. Sturge
Writing, review, and/or revision of the manuscript: M. Rodriguez-Teja, C. Robson, J. Sturge
Administrative, technical, or material support (i.e., reporting or organizing data, constructing databases): M. Rodriguez-Teja, A. Minamidate, J. Waxman, J. Sturge
Study supervision: M. Rodriguez-Teja, J. Waxman, J. Sturge

Acknowledgments

The authors thank Yoshiaki Kawano (Kumamoto University) for technical advice and Isabel Pires (University of Hull) and Catherine Hogan (Cardiff University) for helpful comments during article preparation.

Dedication

This article is dedicated to Peter Gannaway, a good friend, who passed away at age 74 years in December 2012 due to advanced prostate cancer.

Grant Support

This work was supported by grants from The Association of International Cancer Research (grant 08-0803), The Prostate Cancer Charity (grant 110632), The Rosetrees Trust (grants M40/M41), Tony & Rita Gallagher, and Imperial College NHS Healthcare Trust Special Trustees.

The costs of publication of this article were defrayed in part by the payment of page charges. This article must therefore be hereby marked *advertisement* in accordance with 18 U.S.C. Section 1734 solely to indicate this fact.

Received June 18, 2014; revised October 30, 2014; accepted November 1, 2014; published OnlineFirst November 7, 2014.

References

1. Thiery JP, Acloque H, Huang RY, Nieto MA. Epithelial-mesenchymal transitions in development and disease. Cell 2009;139:871–90.
2. Kalluri R, Weinberg RA. The basics of epithelial-mesenchymal transition. J Clin Invest 2009;119:1420–8.
3. Rhim AD, Mirek ET, Aiello NM, Maitra A, Bailey JM, McAllister F, et al. EMT and dissemination precede pancreatic tumor formation. Cell 2012;148: 349–61.
4. Drickamer K. C-type lectin-like domains. Curr Opin Struct Biol 1999;9: 585–90.
5. Kogianni G, Walker MM, Waxman J, Sturge J. Endo180 expression with cofunctional partners MT1-MMP and uPAR-uPA is correlated with prostate cancer progression. Eur J Cancer 2009;45:685–93.
6. Curino AC, Engelholm LH, Yamada SS, Holmbeck K, Lund LR, Molinolo AA, et al. Intracellular collagen degradation mediated by uPARAP/ Endo180 is a major pathway of extracellular matrix turnover during malignancy. J Cell Biol 2005;169:977–85.
7. Wienke D, Davies GC, Johnson DA, Sturge J, Lambros MB, Savage K, et al. The collagen receptor Endo180 (CD280) Is expressed on basal-like breast tumor cells and promotes tumor growth in vivo. Cancer Res 2007;67: 10230–40.
8. Caley MP, Kogianni G, Adamarek A, Gronau JH, Rodriguez-Teja M, Fonseca AV, et al. TGFbeta1-Endo180-dependent collagen deposition is dysregulated at the tumour-stromal interface in bone metastasis. J Pathol 2012; 226:775–83.
9. Huijbers IJ, Iravani M, Popov S, Robertson D, Al-Sarraj S, Jones C, et al. A role for fibrillar collagen deposition and the collagen internalization receptor Endo180 in glioma invasion. PLoS One 2010;5:e9808.
10. Ikenaga N, Ohuchida K, Mizumoto K, Akagawa S, Fujiwara K, Eguchi D, et al. Pancreatic cancer cells enhance the ability of collagen internalization during epithelial-mesenchymal transition. PLoS One 2012;7: e40434.
11. Sturge J, Wienke D, East L, Jones GE, Isacke CM. GPI-anchored uPAR requires Endo180 for rapid directional sensing during chemotaxis. J Cell Biol 2003;162:789–94.
12. Sturge J, Wienke D, Isacke CM. Endosomes generate localized Rho-ROCK-MLC2-based contractile signals via Endo180 to promote adhesion disassembly. J Cell Biol 2006;175:337–47.
13. Gately K, Al-Alao B, Dhillon T, Mauri F, Cuffe S, Seckl M, et al. Overexpression of the mammalian target of rapamycin (mTOR) and angioinvasion are poor prognostic factors in early stage NSCLC: a verification study. Lung Cancer 2012;75:217–22.
14. Wienke D, MacFadyen JR, Isacke CM. Identification and characterization of the endocytic transmembrane glycoprotein Endo180 as a novel collagen receptor. Mol Biol Cell 2003;14:3592–604.
15. Madsen DH, Engelholm LH, Ingvarsen S, Hillig T, Wagenaar-Miller RA, Kjoller L, et al. Extracellular collagenases and the endocytic receptor, urokinase plasminogen activator receptor-associated protein/Endo180, cooperate in fibroblast-mediated collagen degradation. J Biol Chem 2007; 282:27037–45.
16. Zhong WD, Liang YX, Lin SX, Li L, He HC, Bi XC, et al. Expression of CD147 is associated with prostate cancer progression. Int J Cancer 2012; 130:300–8.
17. Tang W, Chang SB, Hemler ME. Links between CD147 function, glycosylation, and caveolin-1. Mol Biol Cell 2004;15:4043–50.
18. Wright JL, Salinas CA, Lin DW, Kolb S, Koopmeiners J, Feng Z, et al. Prostate cancer specific mortality and Gleason 7 disease differences in prostate cancer outcomes between cases with Gleason 4 + 3 and Gleason 3 + 4 tumors in a population based cohort. J Urol 2009;182: 2702–7.
19. Wu J, Ru NY, Zhang Y, Li Y, Wei D, Ren Z, et al. HAb18G/CD147 promotes epithelial-mesenchymal transition through TGF-beta signaling and is transcriptionally regulated by Slug. Oncogene 2011;30: 4410–27.
20. Rucci N, Millimaggi D, Mari M, Del Fattore A, Bologna M, Teti A, et al. Receptor activator of NF-kappaB ligand enhances breast cancer-induced osteolytic lesions through upregulation of extracellular matrix metalloproteinase inducer/CD147. Cancer Res 2010;70:6150–60.
21. Rodriguez-Teja M, Gronau JH, Breit C, Zhang YZ, Caley M, Minamidate A, et al. (2014). AGE modified basement membrane cooperates with Endo180 to promote epithelial cell invasiveness and decrease prostate cancer survival. J Path 2015;235:581–92.
22. Wells RG, Discher DE. Matrix elasticity, cytoskeletal tension, and TGF-beta: the insoluble and soluble meet. Sci Signal 2008;1:pe13.
23. Diener KR, Need EF, Buchanan G, Hayball JD. TGF-beta signalling and immunity in prostate tumourigenesis. Expert Opin Ther Targets 2010;14: 179–92.
24. Zheng H, Kang Y. Multilayer control of the EMT master regulators. Oncogene 2014;33:1755–63.
25. East L, Rushton S, Taylor ME, Isacke CM. Characterization of sugar binding by the mannose receptor family member, Endo180. J Biol Chem 2002; 277:50469–75.
26. Martinez-Pomares L. The mannose receptor. J Leukoc Biol 2012;92: 1177–86.
27. Mura M, Swain RK, Zhuang X, Vorschmitt H, Reynolds G, Durant S, et al. Identification and angiogenic role of the novel tumor endothelial marker CLEC14A. Oncogene 2012;31:293–305.
28. Ki MK, Jeoung MH, Choi JR, Rho SS, Kwon YG, Shim H, et al. Human antibodies targeting the C-type lectin-like domain of the tumor endothelial

cell marker clec14a regulate angiogenic properties in vitro. Oncogene 2013;32:5449–57.
29. Rho SS, Choi HJ, Min JK, Lee HW, Park H, Park H, et al. Clec14a is specifically expressed in endothelial cells and mediates cell to cell adhesion. Biochem Biophys Res Comm 2011;404:103–8.
30. Nanda A, Karim B, Peng Z, Liu G, Qiu W, Gan C, et al. Tumor endothelial marker 1 (Tem1) functions in the growth and progression of abdominal tumors. Proc Nat Acad Sci U S A 2006;103:3351–6.
31. Valdez Y, Maia M, Conway EM. CD248: reviewing its role in health and disease. Curr Drug Targets 2012;13:432–9.
32. East L, McCarthy A, Wienke D, Sturge J, Ashworth A, Isacke CM. A targeted deletion in the endocytic receptor gene Endo180 results in a defect in collagen uptake. EMBO Rep 2003;4:710–6.
33. Engelholm LH, List K, Netzel-Arnett S, Cukierman E, Mitola DJ, Aaronson H, et al. uPARAP/Endo180 is essential for cellular uptake of collagen and promotes fibroblast collagen adhesion. J Cell Biol 2003;160:1009–15.
34. Jurgensen HJ, Madsen DH, Ingvarsen S, Melander MC, Gardsvoll H, Patthy L, et al. A novel functional role of collagen glycosylation: interaction with the endocytic collagen receptor uparap/ENDO180. J Biol Chem 2011; 286:32736–48.
35. Igakura T, Kadomatsu K, Kaname T, Muramatsu H, Fan QW, Miyauchi T, et al. A null mutation in basigin, an immunoglobulin superfamily member, indicates its important roles in peri-implantation development and spermatogenesis. Dev Biol 1998;194:152–65.
36. Eyster CA, Higginson JD, Huebner R, Porat-Shliom N, Weigert R, Wu WW, et al. Discovery of new cargo proteins that enter cells through clathrin-independent endocytosis. Traffic 2009;10:590–9.
37. Iacono KT, Brown AL, Greene MI, Saouaf SJ. CD147 immunoglobulin superfamily receptor function and role in pathology. Exp Mol Path 2007; 83:283–95.
38. Schrecengost R, Knudsen KE. Molecular pathogenesis and progression of prostate cancer. Semin Oncol 2013;40:244–58.
39. Palmieri C, Caley MP, Purshouse K, Fonseca AV, Rodriguez-Teja M, Kogianni G, et al. Endo180 modulation by bisphosphonates and diagnostic accuracy in metastatic breast cancer. Br J Cancer 2012;108: 163–9.

AACR American Association for Cancer Research

Molecular Cancer Research

Survival Outcome and EMT Suppression Mediated by a Lectin Domain Interaction of Endo180 and CD147

Mercedes Rodriguez-Teja, Julian H. Gronau, Ai Minamidate, et al.

Mol Cancer Res 2015;13:538-547. Published OnlineFirst November 7, 2014.